Research Article Vol. 10, No. 8 / August 2023 / Optica 965



Effective electromagnetic wave properties of disordered stealthy hyperuniform layered media beyond the quasistatic regime

JAEUK KIM[1,2,3] AND SALVATORE TORQUATO[1,2,3,4,*]

[1]Department of Chemistry, Princeton University, Princeton, New Jersey 08544, USA
[2]Princeton Materials Institute, Princeton University, Princeton, New Jersey 08544, USA
[3]Department of Physics, Princeton University, Princeton, New Jersey 08544, USA
[4]Program in Applied and Computational Mathematics, Princeton University, Princeton, New Jersey 08544, USA
*torquato@princeton.edu

Received 16 March 2023; revised 19 May 2023; accepted 26 June 2023; published 24 July 2023

Disordered stealthy hyperuniform **dielectric composites exhibit novel electromagnetic wave transport properties in two and three dimensions. Here, we carry out the first study of the electromagnetic properties of one-dimensional 1D) disordered stealthy hyperuniform layered media. From an exact nonlocal theory, we derive an approximation formula for the effective dynamic dielectric constant tensor $\boldsymbol{\varepsilon}_e(\mathbf{k}_q, \omega)$ of general 1D media that is valid well beyond the quasistatic regime and apply it to 1D stealthy hyperuniform systems. We consider incident waves of transverse polarization, frequency ω, and wavenumber k_q. Our formula for $\boldsymbol{\varepsilon}_e(\mathbf{k}_q, \omega)$, which is given in terms of the *spectral density*, leads to a closed-form relation for the transmittance T. Our theoretical predictions are in excellent agreement with finite-difference time-domain (FDTD) simulations. Stealthy hyperuniform layered media have perfect transparency intervals up to a finite wavenumber, implying no Anderson localization, but non-stealthy hyperuniform media are not perfectly transparent. Our predictive theory provides a new path for the inverse design of the wave characteristics of disordered layered media, which are readily fabricated, by engineering their spectral densities.** © 2023 Optica Publishing Group under the terms of the Optica Open Access Publishing Agreement

https://doi.org/10.1364/OPTICA.489797

1. INTRODUCTION

Disordered hyperuniform many-body systems [1–3] are an emerging class of amorphous states of matter that are endowed with novel wave and other transport properties with advantages over their periodic counterparts [3–23]. Such hyperuniform two-phase composites are characterized by an anomalous suppression of volume-fraction fluctuations in the infinite-wavelength limit [2,3], i.e., the local volume-fraction variance $\sigma_V^2(R)$ inside a spherical observation window of radius R decays faster than R^{-d} in d dimensions in the large-R limit, $\lim_{R\to\infty} R^d\sigma_V^2(R) = 0$. Equivalently, its associated *spectral density* $\tilde{\chi}_V(\mathbf{k})$ vanishes as the wavenumber $|\mathbf{k}|$ tends to zero, i.e., $\lim_{|\mathbf{k}|\to 0} \tilde{\chi}_V(\mathbf{k}) = 0$. One important class of such hyperuniform media is the disordered *stealthy* varieties in which $\tilde{\chi}_V(\mathbf{k}) = 0$ for $0 < |\mathbf{k}| < K$ [24–27], meaning that they completely suppress single scattering of incident radiation for these wave vectors [3,25]. The degree of stealthiness χ is the ratio of the number of the constrained wave vectors in the reciprocal space to the total number of degrees of freedom. Recent studies showed that such exotic disordered media exhibit novel electromagnetic wave transport properties, including high transparency in the optically dense regime, maximized absorption, and complete photonic bandgap formation [4,5,7,8,10,12–17,20–23,28–30] in two and three spatial dimensions. For example, previous work on light transparency of stealthy hyperuniform systems considered two-dimensional (2D) point scatterers [7] and 2D and three-dimensional (3D) two-phase dielectric composites [10,31]. Here, we undertake the first study of the electromagnetic properties of one-dimensional (1D) disordered stealthy hyperuniform layered media.

The problem of wave propagation in a two-phase (or multiphase) layered medium has been extensively studied because of its simplicity and its ease of fabrication [32,33], including surface plasmons [34,35], Anderson localization [36–41], and deep-subwavelength disorder [42], as well as practical applications [18,43–45]. An important wave characteristic is the effective dynamic dielectric constant tensor $\boldsymbol{\varepsilon}_e(\mathbf{k}_q, \omega)$ for the incident radiation of frequency ω and wave vector $\mathbf{k}_q$. This complex-valued quantity determines the effective wavenumber k_e and extinction mean free path ℓ_e. While there have been many theoretical/numerical treatments to estimate $\boldsymbol{\varepsilon}_e(\mathbf{k}_q, \omega)$ of layered media [46–53], previous approximations are applicable to disordered media in the *quasistatic* or long-wavelength regime, i.e., $|\mathbf{k}_q|\xi \ll 1$, where ξ is a characteristic inhomogeneity length scale.

Torquato and Kim [31] recently derived the general nonlocal strong-contrast expansion for the effective dielectric constant tensor $\boldsymbol{\varepsilon}_e(\mathbf{k}_q, \omega)$ that can be applied to two-phase media with

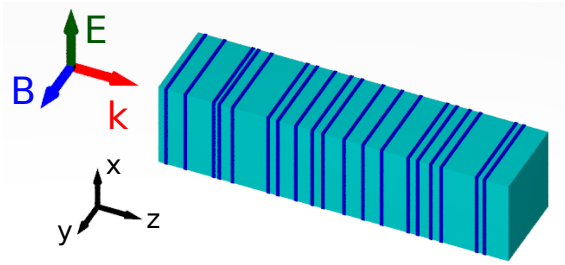


Fig. 1. Schematic of three-dimensional disordered anisotropic stratified media consisting of infinite parallel slabs of phases 1 (cyan) and 2 (dark blue). A plane electromagnetic wave of transverse polarization is normally incident into the medium, and its wave vector is shown as a red arrow.

various symmetries. This expansion exactly treats multiple scattering to all orders beyond the quasistatic regime (i.e., $0 \le |\mathbf{k}_q|\xi \lesssim 1$) as a series involving functionals of the n-point correlation functions $S^{(i)}(\mathbf{x}_1, \ldots, \mathbf{x}_n)$ for all n (Section 2). Here, the quantity $S^{(i)}(\mathbf{x}_1, \ldots, \mathbf{x}_n)$ gives the probability of finding n points at positions $\mathbf{x}_1, \ldots, \mathbf{x}_n$ all in phase i $(= 1, 2)$. Because of the fast-convergence property of this series (or the linear fractional form of this series), truncating it at the n-point level yields *multiple-scattering* approximations that still accurately capture multiple scattering to all orders for a wide class of microstructures, including statistically *anisotropic* media. The second-order truncations already provide accurate approximations for 2D and 3D statistically isotropic two-phase media [31]. However, and importantly, analogous approximations for statistically anisotropic media have yet to be extracted and applied.

Here, we theoretically and numerically investigate the tensor $\boldsymbol{\varepsilon}_e(\mathbf{k}_q, \omega)$ of 3D anisotropic layered media consisting of infinite parallel dielectric slabs of phases 1 and 2 whose thicknesses are derived from 1D disordered stealthy hyperuniform packings at various χ values. For simplicity, we focus on normally incident waves of transverse polarization, where $\mathbf{k}_q = k_q\hat{\mathbf{z}}$ (see Fig. 1); thus, the wavenumber k_q is the independent variable of the effective dielectric constant. From the exact strong-contrast expansion, we derive, for the first time, formulas for $\boldsymbol{\varepsilon}_e(k_q, \omega)$ for 3D anisotropic layered media that accurately account for multiple scattering in terms of the spectral density $\tilde{\chi}_V(\mathbf{k})$, enabling us to probe a wide range of wavenumbers. The quantity $\tilde{\chi}_V(\mathbf{k})$ is the Fourier transform of the autocovariance function $\chi_V(\mathbf{r}) \equiv S_2^{(i)}(\mathbf{r}) - {\phi_i}^2$ [54], where $\mathbf{r} \equiv \mathbf{x}_2 - \mathbf{x}_1$, and it can be measured from scattering experiments [55]. To our knowledge, this expression is the first closed-form formula of $\boldsymbol{\varepsilon}_e(k_q, \omega)$ for general 1D media that applies well beyond the quasistatic regime.

We numerically verify that our derived formula can accurately capture multiple scattering effects due to correlated disorder beyond the quasistatic regime by using finite-difference time-domain (FDTD) simulations. For this purpose, we numerically generate stealthy hyperuniform stratified dielectric two-phase media via a modified collective-coordinate procedure described in [16,31] (Section 3). For dimensionless wavenumbers up to $k_1/\rho \lesssim 1.5$, our predictions indeed show excellent agreement with the real and imaginary parts of the effective dielectric constant as well as transmittance found from FDTD simulations (Sections 4 and 5 of Supplement 1). Notably, our formula predicts that stealthy hyperuniform layered media are perfectly transparent (defined as $\mathrm{Im}[\varepsilon_e(k_q, \omega)] = 0$) up to a finite wavenumber $K_T = K/(2\sqrt{\phi_1\varepsilon_1 + \phi_2\varepsilon_2})$ (i.e., no Anderson localization) in the infinite-volume limit; see Eq. (12). This result is especially remarkable because extended states in 1D disordered systems are more difficult to achieve than in higher dimensions [17,38–41].

We also show that a perfect transparency interval cannot exist in disordered 1D *non-stealthy* media, *hyperuniform* or not, and thus Anderson localization can be present at all wavenumbers. Our results, combined with the methods to generate media with a prescribed spectral density [13,24–26], provide a new inverse-design approach [56] to engineer and fabricate multilayered dielectric media with novel wave properties.

2. THEORY

A. Exact Strong-Contrast Expansion

Here, we briefly summarize the general nonlocal strong-contrast-expansion formalism of the effective dynamic dielectric constant tensor $\boldsymbol{\varepsilon}_e(\mathbf{k}_q, \omega)$ for 3D two-phase media with arbitrary symmetries [31]. (The strong-property-fluctuation theory [57,58] corresponds to a special case of our strong-contrast formalism, as detailed in Section 1 of Supplement 1.) We consider a macroscopically large two-phase composite specimen in three dimensions embedded inside an infinitely large reference phase q [31,59]. For simplicity, we take the phase q to be the matrix phase (i.e., $q = 1, 2$) and assume that phase 1 and 2 are nonmagnetic and dielectrically isotropic with real-valued and frequency-independent dielectric constants. These assumptions imply the linear dispersion relation in the reference phase [i.e., $k_q(\omega) \equiv |\mathbf{k}_q(\omega)| = \sqrt{\varepsilon_q}\omega/c$], where c is the speed of light in vacuum; thus, we henceforth do not explicitly indicate the ω dependence.

The general nonlocal strong-contrast expansion is a series expansion of the linear fractional form of the tensor $\boldsymbol{\varepsilon}_e(\mathbf{k}_q)$, given as

$$\phi_p \boldsymbol{L}_p^{(q)} \cdot \left(\left\{ \boldsymbol{I} + \boldsymbol{D}^{(q)} \cdot \left[\boldsymbol{\varepsilon}_e(\mathbf{k}_q) - \varepsilon_q \boldsymbol{I} \right] \right\} \cdot \left[\boldsymbol{\varepsilon}_e(\mathbf{k}_q) - \varepsilon_q \boldsymbol{I} \right]^{-1} \right) \cdot \phi_p \boldsymbol{L}_p^{(q)}$$
$$= \phi_p \boldsymbol{L}_p^{(q)} - \sum_{n=2}^{\infty} \mathcal{A}_n^{(p)}(\mathbf{k}_q), \tag{1}$$

where $p (\neq q)$ indicates the polarized phase, $\boldsymbol{L}_p^{(q)}$ is the expansion parameter defined as

$$\boldsymbol{L}_p^{(q)} \equiv (\varepsilon_p - \varepsilon_q)\left[\boldsymbol{I} + \boldsymbol{D}^{(q)}(\varepsilon_p - \varepsilon_q) \right]^{-1}, \tag{2}$$

and $\mathcal{A}_n^{(p)}(\mathbf{k}_q)$ is a wave-vector-dependent second-rank tensor that is a functional involving the set of correlation functions $S_1^{(p)}, S_2^{(p)}, \ldots, S_n^{(p)}$ and products of the principal part of the dyadic Green's function $\boldsymbol{H}^{(q)}(\mathbf{r})$; see Section 1 of Supplement 1. The series expansion [Eq. (1)] has four salient features. First, Eq. (1) is derived from a spatially nonlocal averaged constitutive relation [50,60,61], resulting in an expansion that is valid from the long- to intermediate-wavelength regimes. Second, Eq. (1) exactly treats multiple scattering to all orders at a given incident wave vector $\mathbf{k}_q$ when the nonlocal homogenization theory is valid because the terms $\mathcal{A}_n^{(p)}(\mathbf{k}_q)$ for $n = 2, \ldots$ in Eq. (1) explicitly account for complete microstructural information (the infinite set of S_2, S_3, …) to infinite order [31]; see Section 1 of Supplement 1

for details. Third, the choice of the shape of the infinitesimal exclusion region (i.e., $\boldsymbol{D}^{(q)}$) leads to a different expansion parameter $\boldsymbol{L}_p^{(q)}$ that determines the convergence properties. Thus, unlike standard multiple-scattering theories [38,62,63], here one can naturally "tune" the general series expansion to obtain distinctly different approximations suited for certain classes of microstructures. Fourth, the left side of the series [Eq. (1)] is a linear fractional transformation of $\boldsymbol{\varepsilon}_e(\mathbf{k}_q)$ rather than $\boldsymbol{\varepsilon}_e(\mathbf{k}_q)$ itself, which leads to the rapid convergence of the strong-contrast expansions so that its lower-order truncations approximate well higher-order functionals (i.e., multiple scattering) of the exact series to all orders in terms of lower-order diagrams [31].

B. Multiple-Scattering Approximations for Layered Media

We can now extract from the exact strong-contrast expansion [Eq. (1)] accurate multiple-scattering approximations for layered media by truncating the expansion at the n-point level. We focus here on such a formula at the two-point level that depends on the spectral density $\tilde{\chi}_V(\mathbf{k})$ because it is still accurate and easy to compute. For simplicity, we restrict ourselves to normally incident waves (Fig. 1); thus, the effective dielectric constant now depends on the wavenumber k_q. We outline the derivation here and provide details in Section 2 of Supplement 1.

Since layered media have rotational symmetry about the z axis and translational symmetry in the $x-y$ plane, the spectral density can be expressed as

$$\tilde{\chi}_V(\mathbf{k}) = (2\pi)^2\delta(k_x)\delta(k_y)\tilde{\chi}_V(k_z), \tag{3}$$

where $\delta(k)$ is the 1D Dirac delta function, and $\tilde{\chi}_V(k_z)$ is the spectral density of 1D two-phase media. For 1D packings of identical hard rods of radius a and packing fraction ϕ_2, $\tilde{\chi}_V(k_z) = \phi_2[2\sin^2(k_z a)]/(k_z^2 a)S(k_z)$ [54,64], where $S(k_z)$ is the structure factor of the rod centers. Due to these symmetries, when applying the series [Eq. (1)] to layered media, we utilize the feature 3 discussed in Section 2.A by choosing a disk-like exclusion region normal to the z axis [31], leading to

$$\boldsymbol{D}^{(q)} = \varepsilon_q^{-1}\hat{\mathbf{z}}\hat{\mathbf{z}}, \quad \boldsymbol{L}_p^{(q)} = \beta_{pq}[\varepsilon_p(\boldsymbol{I} - \hat{\mathbf{z}}\hat{\mathbf{z}}) + \varepsilon_q\hat{\mathbf{z}}\hat{\mathbf{z}}], \tag{4}$$

where $\hat{\mathbf{z}}$ is a unit vector along the z direction and β_{pq} is the 1D counterpart of the *dielectric polarizability*, defined as $\beta_{pq} \equiv 1 - \varepsilon_q/\varepsilon_p$. Here, $\boldsymbol{L}_p^{(q)}$ is obtained by substituting $\boldsymbol{D}^{(q)}$ in Eq. (4) into Eq. (2). Using Eq. (4) and the assumption of normal incidence, the general expression for $\mathcal{A}_2^{(p)}(k_q)$ simplifies as

$$\mathcal{A}_2^{(p)}(k_q) = (\varepsilon_p\beta_{pq})^2\frac{F^{(1D)}(k_q)}{\varepsilon_q}(\boldsymbol{I} - \hat{\mathbf{z}}\hat{\mathbf{z}}), \tag{5}$$

$$F^{(1D)}(k) = \frac{k^2}{\pi}\text{p.v.}\int_0^\infty dq_z\frac{\tilde{\chi}_V(q_z)}{q_z^2 - (2k)^2} + \frac{ik}{4}[\tilde{\chi}_V(0) + \tilde{\chi}_V(2k)], \tag{6}$$

where p.v. stands for the Cauchy principal value. Note that $F^{(1D)}(k_q)$ is the nonlocal attenuation function for 1D two-phase media, whose 2D and 3D counterparts were derived in [31].

Applying Eq. (4) and Eq. (5) into the second-order truncation of the series [Eq. (1)] yields

$$\frac{(\phi_p\varepsilon_p\beta_{pq})^2}{\varepsilon_q(\varepsilon_e^\perp(k_q)/\varepsilon_q - 1)}(\boldsymbol{I} - \hat{\mathbf{z}}\hat{\mathbf{z}}) + \frac{(\phi_p\varepsilon_q\beta_{pq})^2}{\varepsilon_q(1 - \varepsilon_q/\varepsilon_e^z(k_q))}\hat{\mathbf{z}}\hat{\mathbf{z}}$$
$$= \varepsilon_p\beta_{pq}[\phi_p - (\varepsilon_p\beta_{pq})F^{(1D)}(k_q)/\varepsilon_q](\boldsymbol{I} - \hat{\mathbf{z}}\hat{\mathbf{z}}) + \phi_p\varepsilon_q\beta_{pq}\hat{\mathbf{z}}\hat{\mathbf{z}}, \tag{7}$$

where we have decomposed the effective dielectric constant tensor into two orthogonal components $\varepsilon_e^\perp(k_q)$ and $\varepsilon_e^z(k_q)$ for the transverse and longitudinal polarizations, respectively, as follows: $\boldsymbol{\varepsilon}_e(\mathbf{k}_q) = \varepsilon_e^\perp(k_q)(\boldsymbol{I} - \hat{\mathbf{z}}\hat{\mathbf{z}}) + \varepsilon_e^z(k_q)\hat{\mathbf{z}}\hat{\mathbf{z}}$. Now Eq. (7) provides two independent approximations:

$$\varepsilon_e^\perp(k_q) = \varepsilon_q\left[1 + \frac{\phi_p^2(\varepsilon_p/\varepsilon_q)\beta_{pq}}{\phi_p - (\varepsilon_p\beta_{pq})F^{(1D)}(k_q)/\varepsilon_q}\right], \tag{8}$$

$$\varepsilon_e^z(k_q) = \varepsilon_q(1 - \phi_p\beta_{pq})^{-1}. \tag{9}$$

Note that $\varepsilon_e^\perp(k_q)$ is dependent on the incident wavenumber k_q and is complex-valued if $\tilde{\chi}_V(0) + \tilde{\chi}_V(2k_q) > 0$, implying that the media can be lossy due to forward scattering and backscattering from inhomogeneties in the local dielectric constant. By contrast, $\varepsilon_e^z(k_q)$ is independent of k_q, reflecting the fact that a traveling longitudinal wave cannot exist under our assumptions. Hence, we focus on $\varepsilon_e^\perp(k_q)$ in the rest of this work. In the static limit, Eqs. (8) and (9) reduce to the arithmetic and harmonic means of the dielectric constants, respectively,

$$\varepsilon_e^\perp(0) = \langle\varepsilon\rangle \equiv \phi_p\varepsilon_p + \phi_q\varepsilon_q, \quad \varepsilon_e^z(0) = (\phi_p/\varepsilon_p + \phi_q/\varepsilon_q)^{-1}. \tag{10}$$

Interestingly, these static results are exact for any microstructure [54]. Renormalization of the reference phase for the optimal convergence (Section 2 of Supplement 1), equivalent to using the effective Green's function in [31], yields a *scaled* strong-contrast approximation for disordered layered media,

$$\varepsilon_e^\perp(k_q) = \varepsilon_q\left[1 + \frac{\phi_p^2(\varepsilon_p/\varepsilon_q)\beta_{pq}}{\phi_p - (\varepsilon_p\beta_{pq})F^{(1D)}\left(k_q\sqrt{\langle\varepsilon\rangle/\varepsilon_q}\right)/\langle\varepsilon\rangle}\right], \tag{11}$$

where $\langle\varepsilon\rangle$ is given in Eq. (10). We henceforth focus on this scaled approximation because it is more accurate than Eq. (8), as shown Fig. S6 in Supplement 1. As shown in [31], Eq. (11) satisfies the Kramers–Kronig relations [65] so that its predictions properly exhibit both *normal dispersion* [i.e., an increase in $\text{Re}[\varepsilon_e^\perp]$ with k_q] and *anomalous dispersion* [i.e., a decrease in $\text{Re}[\varepsilon_e^\perp]$ with k_q]. Furthermore, satisfying the Kramers–Kronig relations also implies that Eq. (11) yields qualitatively accurate predictions, even beyond the validity regime (i.e., $k_q/\rho \lesssim 1.5$); see Sections 5 and 6 in Supplement 1 for details.

In the scaled approximation [Eq. (11)], the quantity $F^{(1D)}(k_q)$ is generally complex-valued at a given incident wavenumber k_q, producing a corresponding $\varepsilon_e^\perp(k_q)$ with a nonnegative imaginary part. Following conventional usage, a composite attenuates waves at a given wavenumber if the imaginary part of the effective dielectric constant is positive. Such attenuation occurs here only because of multiple scattering effects (not absorption).

Importantly, our strong-contrast approximation [Eq. (11)] predicts that stealthy hyperuniform layered media can be perfectly transparent (i.e., $\text{Im}[\varepsilon_e^\perp] = 0$) in the infinite-volume limit for a finite range of wavenumbers. Since any stealthy hyperuniform systems completely suppress both forward scattering and backscattering [i.e., $\tilde{\chi}_V(0) + \tilde{\chi}_V(2k_1) = 0$] for $k_1 < K/2$,

$\mathrm{Im}[F^{(1D)}(k_1)] = 0$, and substituting this condition into the scaled formula [Eq. (11)] yields a perfect transparency interval,

$$0 \le k_1 < K_T \equiv \frac{K}{2\sqrt{\langle\varepsilon\rangle}} = \frac{\rho\pi\chi}{\sqrt{\langle\varepsilon\rangle}}, \tag{12}$$

where $\langle\varepsilon\rangle$ is the arithmetic mean of the local dielectric constant; see Eq. (10). Perfect transparency implies an infinite localization length within this spectral range, which is consistent with an estimate that the localization length is inversely proportional to what we call the spectral density [40]. We stress that the prediction [Eq. (12)] is purely theoretical and, hence, does not rely on simulations or measurements of the spectral density.

3. MODEL MICROSTRUCTURES

Stealthy hyperuniform particle systems are defined by a spectral density that vanishes in a finite range of wavenumbers that includes the origin [$\tilde{\chi}_V(\mathbf{k}) = 0$ for $0 < |\mathbf{k}| \le K$]. The degree of stealthiness χ is measured by the ratio of the number of the constrained wave vectors in the reciprocal space to the total degrees of freedom, i.e., in one dimension, $\chi = K/(2\pi\rho)$, where ρ is the number density of particles. For $\chi < 0.5$ in two and three dimensions or $\chi < 1/3$ in one dimension, these stealthy hyperuniform systems are highly degenerate and disordered [26]. Thus, we consider 1D cases in which χ takes the following values: $\chi = 0.1, 0.2, 0.3$. Henceforth, we take the characteristic inhomogeneity length scale ξ to be the mean particle separation $1/\rho$, which is of the order of the mean nearest-neighbor distance ℓ_P, (i.e., $\ell_P \sim 1/\rho$). This choice means that the range of validity of our nonlocal theory is $k_1/\rho \lesssim 1.5$ for the current models, as shown later in Section 5.

We numerically generate 1D packings of packing fraction $\phi_2 = 0.2$ in the following two-step procedure. First, we generate point configurations of N particles in a periodic fundamental cell $\mathfrak{F}$ via the *collective-coordinate optimization* technique [24–26], which numerically generates ground states with very high-precision of the following potential energy:

$$\Phi(\mathbf{r}^N) = \frac{1}{V_{\mathfrak{F}}} \sum_{|\mathbf{k}|<K} \tilde{v}(\mathbf{k}) S(\mathbf{k}) + \sum_{i<j} u(r_{ij}), \tag{13}$$

where $\tilde{v}(\mathbf{k}) = 1$ for $|\mathbf{k}| < K$, $V_{\mathfrak{F}}$ is the volume of $\mathfrak{F}$, and a soft-core repulsion term [66] is

$$u(r) = \begin{cases} (1 - r/\sigma)^2, & r < \sigma, \\ 0, & \text{otherwise.} \end{cases} \tag{14}$$

The soft repulsion [Eq. (14)] is to get the stealthy hyperuniform ground states whose nearest-neighbor distances are larger than the length scale σ [16,31]. Finally, we create packings with dielectric constant ε_2 by circumscribing the points by identical rods of radius $a < \sigma/2$ without overlaps [8]; see Fig. 2(a). The parameters used to generate these systems are listed in Section 3 of Supplement 1.

We compute the spectral density $\tilde{\chi}_V(k)$ from the generated packings as shown in Fig. 2(b). From the long- to intermediate-wavelength regimes ($k/\rho \lesssim 10$), we clearly see that stealthy hyperuniform packings exhibit a higher degree of correlations as χ increases. In the small-wavelength regime ($k/\rho \gg 10$ or, equivalently, $ka \gg 1$), however, the curves tend to collapse onto a single curve, reflecting the fact that these three systems consist of identical hard rods.

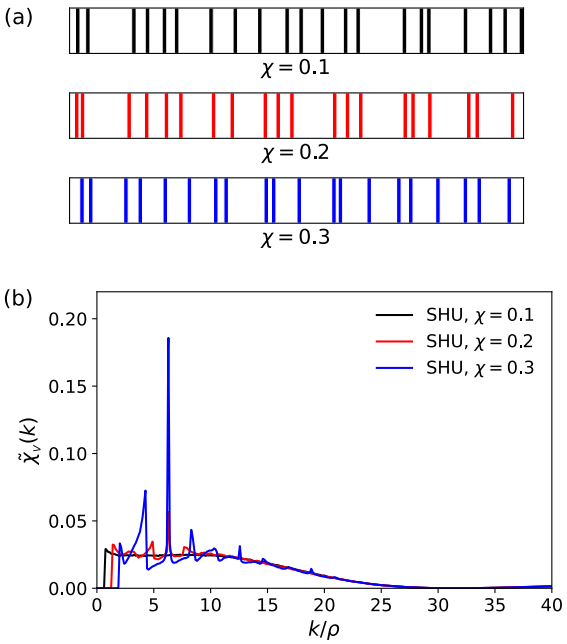


Fig. 2. Disordered stealthy hyperuniform layered media of packing fraction $\phi_2 = 0.2$ and unit number density $\rho = 1$ at three values of $\chi = 0.1, 0.2, 0.3$. (a) Representative images at $\chi = 0.1$ (top), $\chi = 0.2$ (middle), and $\chi = 0.3$ (bottom). The particle phases are shown in different colors. (b) Spectral densities $\tilde{\chi}_V(k)$ as functions of dimensionless wavenumber k/ρ.

4. SIMULATIONS

We validate the accuracy of our predictions on the effective dielectric constant $\varepsilon_e^{\perp}(k_1)$ and the transmittance T by comparing primarily to full-waveform simulations [67] via an open-source FDTD package MEEP [68], although we use the transfer matrix method to compute T, as explained in Supplement 1. We take the matrix to be the reference phase (i.e., $q = 1$) and the particles to be the polarized phase (i.e., $p = 2$) and set the phase contrast ratio as $\varepsilon_2/\varepsilon_1 = 4$. We measure the transmittance spectra T through the disordered stealthy hyperuniform layered media, which are then compared to the predictions from Eq. (11). We also directly extract $\varepsilon_e^{\perp}(k_1)$ from the nonlocal constitutive relation $\varepsilon_e^{\perp}(k_1) = \langle\tilde{D}(k_e,\omega)\rangle/\langle\tilde{E}(k_e,\omega)\rangle$ at a given frequency ω, as was done in [31]; see Fig. S6 of Supplement 1. Here, $\langle\tilde{D}(k_e,\omega)\rangle$ and $\langle\tilde{E}(k_e,\omega)\rangle$ are the spatial Fourier transforms of the ensemble averages of dielectric displacement field $\langle D(x,\omega)\rangle$ and electric field $\langle E(x,\omega)\rangle$ at the complex-valued *effective wavenumber* k_e, respectively; see details in Section 3 of Supplement 1.

5. RESULTS

We now show how our multiple-scattering approximation [Eq. (11)] enables us to accurately predict the real and imaginary parts of the effective dielectric constant tensor $\boldsymbol{\varepsilon}_e(k_1)$ for disordered stealthy hyperuniform layered media for $\chi = 0.1$, 0.2, and 0.3. We begin by computing the nonlocal attenuation function $F^{(1D)}(k)$ given in Eq. (6) from $\tilde{\chi}_V(k)$; see Fig. 3. Stealthy hyperuniform layered media can achieve $\mathrm{Im}[F^{(1D)}(k)] = 0$ up to a finite wavenumber k, leading to the prediction of perfect transparency interval; see Eq. (12).

Using the values of $F^{(1D)}(k)$ in Fig. 3, we then compute the scaled approximation [Eq. (11)] for $\varepsilon_e^{\perp}(k_1)$; see Fig. 4. Both real

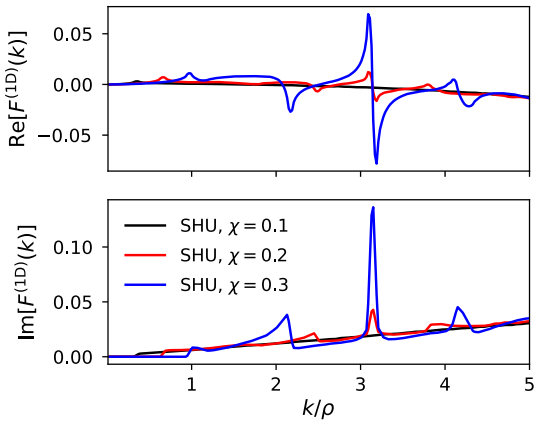


Fig. 3. Real (upper) and imaginary (lower) parts of the nonlocal attenuation functions $F^{(1D)}(k)$ as functions of dimensionless wavenumber k/ρ for 1D disordered stealthy hyperuniform layered media of packing fraction $\phi_2 = 0.2$ at three values of $\chi = 0.1, 0.2, 0.3$. The functions are computed from the spectral densities in Fig. 2 and Eq. (6).

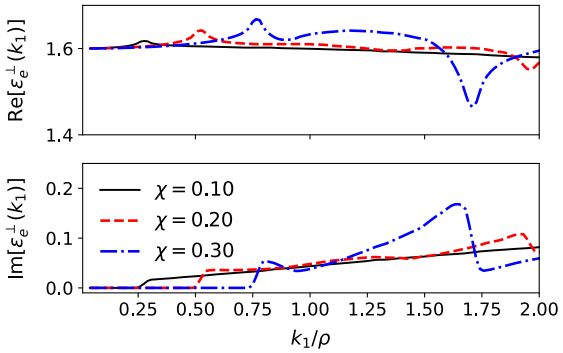


Fig. 4. Predictions of the scaled strong-contrast approximation [Eq. (11)] of the effective dynamic dielectric constant $\varepsilon_e^{\perp}(k_1)$ as a function of the dimensionless incident wavenumber k_1/ρ for disordered stealthy hyperuniform layered media of $\phi_2 = 0.2$ and $\varepsilon_2/\varepsilon_1 = 4$ at $\chi = 0.1, 0.2, 0.3$. The lower panel is a semilog plot of the imaginary part Im[$\varepsilon_e^{\perp}(k_1)$]. For the effective dielectric constants, our theory is accurate up to $k_1/\rho \lesssim 1.5$; see Fig. S6 of Supplement 1.

and imaginary parts of these predictions show excellent agreement with the results from FDTD simulations up to $k_1/\rho \lesssim 1.5$ (see Fig. S6 of Supplement 1). In Fig. 4, the real part of our formula increases with k_1 (normal dispersion) within the perfect transparency interval and then decreases with k_1 (anomalous dispersion) outside of those intervals. Such a spectral dependence of Re[$\varepsilon_e^{\perp}(k_1)$] comes from the fact that the strong-contrast formula satisfies the Kramers–Kronig relations [65] (see Section 6 of Supplement 1), as does the corresponding approximation for 3D statistically isotropic media [31]. Equation (11) also shows qualitatively accurate dielectric responses even beyond the intermediate-wavelength regime (i.e., $k_1/\rho \gtrsim 1.5$) because the Kramers–Kronig relations closely relate the high-frequency predictions of Re[$\varepsilon_e^{\perp}$] to the accurate predictions of Im[$\varepsilon_e^{\perp}$] in a finite spectral range and vice versa [69].

As shown in Fig. 4, these composites are perfectly transparent (i.e., Im[$\varepsilon_e^{\perp}$] = 0) for a wide range of frequencies, as predicted by Eq. (12). At the edges of these transparency intervals, a discontinuous change occurs in Im[$\varepsilon_e^{\perp}$] with k_1 because the imaginary part is directly proportional to $\tilde{\chi}_V(2k_1)$; see Im[$F^{(1D)}(k)$] given

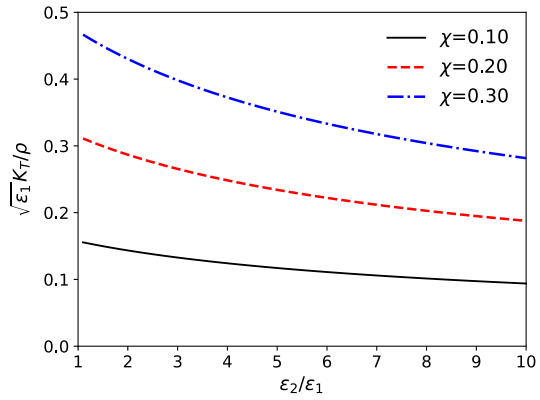


Fig. 5. Prediction [Eq. (12)] of the upper bound K_T of the perfect transparency intervals of 1D stealthy hyperuniform layered media with $\phi_2 = 0.2$ and $\rho = 1$ as a function of the phase contrast ratio $\varepsilon_2/\varepsilon_1$. We consider three χ values: $\chi = 0.1$, 0.2, and 0.3.

in Eq. (6). In higher dimensions, however, such abrupt transitions become increasingly more difficult to achieve, as observed in [31]; see Section 2 of Supplement 1 for detail. Figure 5 depicts how the predicted perfect transparency interval from Eq. (12) varies with the phase contrast ratio $\varepsilon_2/\varepsilon_1$ for given values of χ, ϕ_2, and ρ. We numerically demonstrate that these predicted intervals are valid for $1 < \varepsilon_2/\varepsilon_1 < 10$; see Fig. S3 of Supplement 1.

From our scaled approximation [Eq. (11)], we also predict the *normal* transmittance T through a layered medium at k_1 by assuming that the system is a homogeneous slab of thickness L with an effective dielectric constant $\varepsilon_e^{\perp}(k_1)$ and is optically thin so that waves inside it can interfere coherently. To estimate T, we use an Airy formula [46] of transmittance for a lossy homogeneous slab with absorption:

$$T = \left| \frac{-\sqrt{\varepsilon_e^{\perp}} t^2 \exp(i\sqrt{\varepsilon_e^{\perp}} k_1 L)}{1 - r^2 \exp(2i\sqrt{\varepsilon_e^{\perp}} k_1 L)} \right|^2, \tag{15}$$

where $r \equiv (1 - \sqrt{\varepsilon_e^{\perp}})/(1 + \sqrt{\varepsilon_e^{\perp}})$ and $t \equiv 2/(1 + \sqrt{\varepsilon_e^{\perp}})$, and $\varepsilon_e^{\perp}$ is given by the approximation [Eq. (11)]; see Section 4 of Supplement 1 for results from Eq. (8). The electric field inside the dielectric layered media attenuates solely due to multiple scattering, but its effective behavior is identical to an exponentially damped wave due to absorption in a lossy homogeneous medium (see Fig. S2 of Supplement 1). Hence, we expect Eq. (15) to provide a good approximation of T.

We now compare our theoretical predictions for transmission to the corresponding results obtained from FDTD simulations; see Fig. 6. Remarkably, our theory very accurately predicts the perfect transparency intervals [Eq. (12)], i.e., no Anderson localization (green regions in Fig. 6), because they correctly incorporate multiple scattering at finite wavelengths via the spectral density. This observation is noteworthy because extended states in 1D disordered systems are much more difficult to achieve than in higher dimensions [17,38,39,41]. Within these transparency intervals ($k_1 < K_T$), our theory accurately predicts the small-amplitude periodic oscillations in T around unity, which come from coherent interference of the multiply reflected waves due to the finite system thickness L and, thus, reduce to a constant close to unity when L is much larger than the coherence length of light [46,70]. Outside of the perfect transparency intervals, where scattering attenuation is strong, T from the Airy formula [Eq. (15)] provides

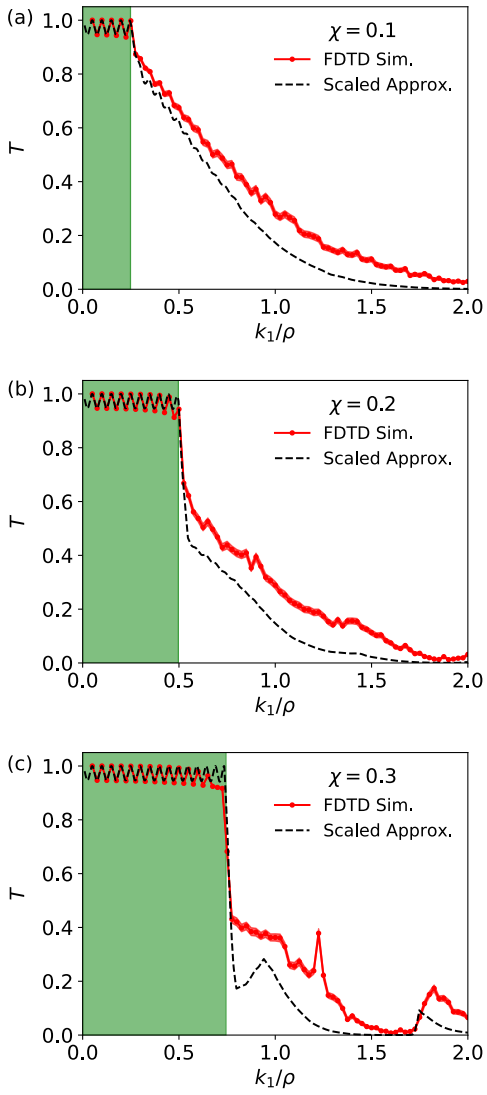


Fig. 6. Transmittance spectra T as a function of the dimensionless wavenumber k_1/ρ for disordered stealthy hyperuniform layered media of packing fraction $\phi_2 (\equiv 2\rho a) = 0.2$ and phase-contrast ratio $\varepsilon_2/\varepsilon_1 = 4$ at three values of (a) $\chi = 0.1$, (b) $\chi = 0.2$, and (c) $\chi = 0.3$. The predictions are computed from Eq. (15) using the scaled approximation [Eq. (11)]. The green-shaded area indicates the predicted transparency intervals [Eq. (12)]. Within these intervals, our predictions show excellent agreement with simulations, since there is no absorption.

a lower bound on the simulation results for the reason explained in Section 4 of Supplement 1. However, we confirm that our theory still accurately predicts, qualitatively, the spectral dependence of T because Eq. (11) yields a physically feasible dielectric response due to the Kramers–Kronig relations. Within these strong-attenuation intervals, T is increasingly suppressed as L increases and becomes virtually zero for sufficiently large L since $\mathrm{Im}[\varepsilon_e^{\perp}(k_1)] > 0$ if $k_1 > K_T$. Stealthy hyperuniformity is required for disordered layered media to possess perfect transparency for a finite range of wavenumbers. Indeed, we show that such a perfect transparency interval cannot exist for "non-stealthy" hyperuniform 1D media, even though these correlated disordered systems anomalously suppress large-scale volume-fraction fluctuations; see the example in Section 7 of Supplement 1.

6. CONCLUSION AND DISCUSSION

In summary, we have theoretically and numerically investigated the effective wave properties, including the effective dynamic dielectric constant tensor $\boldsymbol{\varepsilon}_e(k_q) = \varepsilon_e^{\perp}(k_q)(\boldsymbol{I} - \hat{\boldsymbol{z}}\hat{\boldsymbol{z}}) + \varepsilon_e^{z}(k_q)\hat{\boldsymbol{z}}\hat{\boldsymbol{z}}$ and transmittance T, of 3D statistically anisotropic two-phase layered media made of 1D disordered stealthy hyperuniform packings. To predict $\boldsymbol{\varepsilon}_e(k_q)$ of such exotic disordered models, we derived for the first time a multiple-scattering approximation [Eq. (11)] for statistically anisotropic media from the strong-contrast-expansion formalism. Predictions of both the effective dielectric constant $\varepsilon_e^{\perp}(k_q)$ and transmittance T are in excellent agreement with corresponding results obtained from the FDTD simulations up to $k_1/\rho \lesssim 1.5$. Remarkably, our predictions of T are virtually identical to the simulation results within the perfect transparency ranges. Our multiple-scattering approximation is the first closed-form formula that provides a simple but accurate relation between the effective wave properties of 3D layered media and their spectral density that applies well beyond the quasistatic regime. Beyond the valid range ($k_1/\rho \gtrsim 1.5$), Eq. (11) can still provide qualitatively accurate and physically realistic predictions of dielectric responses since it satisfies the Kramers–Kronig relations.

We applied this newly derived formula [Eq. (11)] to disordered stealthy hyperuniform layered media at $\chi = 0.1$, 0.2, and 0.3. It is noteworthy that our multiple-scattering formula [Eq. (11)] predicts that these disordered systems are perfectly transparent in the infinite-volume limit for a finite ratio $\varepsilon_2/\varepsilon_1$, implying no Anderson localization up to a finite wavenumber proportional to χ, as given by Eq. (12). This observation is remarkable in that such extended states in 1D disordered systems are more difficult to achieve than in higher dimensions [17,38–41]. If the localization length is actually finite, we expect that it will be extremely large for sufficiently small $\varepsilon_2/\varepsilon_1$ compared to any practically large sample size in the transparency interval in such stratified media, as will be reported elsewhere [71]. In contrast, for disordered non-stealthy layered media, hyperuniform or not, our theory shows that there is no spectral range of perfect transparency, implying that localization emerges as the system size grows.

Our findings also have important practical implications. For example, we clearly demonstrate that disordered stealthy hyperuniform layered media can be employed as low-pass filters that transmit waves up to a selected wavenumber. Furthermore, combining our theory with the capabilities to generate media with a prescribed spectral density [13,24–26] enables an inverse-design approach [56] to engineer and fabricate layered dielectric materials with novel wave properties. One possible design is a layered medium satisfying $\tilde{\chi}_V(k) = 0$ for $k < \varepsilon$ and $2k_L < k < 2k_U$, which transmits waves within a narrow spectrum $k_L < k_1 < k_U$. Notably, such computationally designed layered media as well as other 1D disordered models can be readily fabricated via vacuum deposition [72], spin-coating [73], and 3D printing techniques [74]. Thus, our results offer promising prospects for engineering novel optoelectronic devices.

We note that our formalism can be extended to cases of obliquely incident wave vectors $\mathbf{k}_q$, in which both effective dielectric constants $\varepsilon_e^{\perp}(\mathbf{k}_q)$ and $\varepsilon_e^{z}(\mathbf{k}_q)$ become important. Moreover, it also will be interesting to extend our theory to lossy dielectric or metallic phases whose dielectric constants are now frequency-dependent and complex-valued.

Funding. Army Research Office (W911NF-22-2-0103).

Acknowledgment. The authors thank Michael Klatt for helpful discussions. Simulations were performed on computational resources managed and supported by the Princeton Institute for Computational Science and Engineering (PICSciE).

Disclosures. The authors declare no conflicts of interest.

Data availability. Data underlying the results presented in this paper are not publicly available at this time but may be obtained from the authors upon reasonable request.

Supplemental document. See Supplement 1 for supporting content.

REFERENCES

1. S. Torquato and F. H. Stillinger, "Local density fluctuations, hyperuniform systems, and order metrics," Phys. Rev. E **68**, 041113 (2003).
2. C. E. Zachary and S. Torquato, "Hyperuniformity in point patterns and two-phase heterogeneous media," J. Stat. Mech. Theory Exp. **2009**, P12015 (2009).
3. S. Torquato, "Hyperuniform states of matter," Phys. Rep. **745**, 1–95 (2018).
4. M. Florescu, S. Torquato, and P. J. Steinhardt, "Designer disordered materials with large complete photonic band gaps," Proc. Natl. Acad. Sci. USA **106**, 20658–20663 (2009).
5. W. Man, M. Florescu, E. P. Williamson, Y. He, S. R. Hashemizad, B. Y. C. Leung, D. R. Liner, S. Torquato, P. M. Chaikin, and P. J. Steinhardt, "Isotropic band gaps and freeform waveguides observed in hyperuniform disordered photonic solids," Proc. Natl. Acad. Sci. USA **110**, 15886–15891 (2013).
6. T. Ma, H. Guerboukha, M. Girard, A. D. Squires, R. A. Lewis, and M. Skorobogatiy, "3D printed hollow-core terahertz optical waveguides with hyperuniform disordered dielectric reflectors," Adv. Opt. Mater. **4**, 2085–2094 (2016).
7. O. Leseur, R. Pierrat, and R. Carminati, "High-density hyperuniform materials can be transparent," Optica **3**, 763–767 (2016).
8. G. Zhang, F. H. Stillinger, and S. Torquato, "Transport, geometrical, and topological properties of stealthy disordered hyperuniform two-phase systems," J. Chem. Phys. **145**, 244109 (2016).
9. Y. Xu, S. Chen, P.-E. Chen, W. Xu, and Y. Jiao, "Microstructure and mechanical properties of hyperuniform heterogeneous materials," Phys. Rev. E **96**, 043301 (2017).
10. L. Froufe-Pérez, M. Engel, J. Sáenz, and F. Scheffold, "Band gap formation and Anderson localization in disordered photonic materials with structural correlations," Proc. Natl. Acad. Sci. USA **114**, 9570–9574 (2017).
11. M. A. Klatt and S. Torquato, "Characterization of maximally random jammed sphere packings. III. Transport and electromagnetic properties via correlation functions," Phys. Rev. E **97**, 012118 (2018).
12. S. Torquato, "Extraordinary disordered hyperuniform multifunctional composites," J. Compos. Mater. **56**, 3635–3649 (2022).
13. D. Chen and S. Torquato, "Designing disordered hyperuniform two-phase materials with novel physical properties," Acta Mater. **142**, 152–161 (2018).
14. H. Zhang, W. Wu, and Y. Hao, "Luneburg lens from hyperuniform disordered composite materials," in *IEEE International Symposium on Antennas and Propagation and USNC/URSI National Radio Science Meeting* (2018), pp. 2281–2282.
15. S. Gorsky, W. A. Britton, Y. Chen, J. Montaner, A. Lenef, M. Raukas, and L. Dal Negro, "Engineered hyperuniformity for directional light extraction," APL Photon. **4**, 110801 (2019).
16. J. Kim and S. Torquato, "Multifunctional composites for elastic and electromagnetic wave propagation," Proc. Natl. Acad. Sci. USA **117**, 8764–8774 (2020).
17. S. Yu, C.-W. Qiu, Y. Chong, S. Torquato, and N. Park, "Engineered disorder in photonics," Nat. Rev. Mater. **6**, 226–243 (2021).
18. V. Romero-García, É. Chéron, S. Kuznetsova, J.-P. Groby, S. Félix, V. Pagneux, and L. M. Garcia-Raffi, "Wave transport in 1D stealthy hyperuniform phononic materials made of non-resonant and resonant scatterers," APL Mater. **9**, 101101 (2021).
19. F. Sgrignuoli, S. Torquato, and L. Dal Negro, "Subdiffusive wave transport and weak localization transition in three-dimensional stealthy hyperuniform disordered systems," Phys. Rev. B **105**, 064204 (2022).
20. N. Granchi, R. Spalding, M. Lodde, M. Petruzzella, F. W. Otten, A. Fiore, F. Intonti, R. Sapienza, M. Florescu, and M. Gurioli, "Near-field investigation of luminescent hyperuniform disordered materials," Adv. Opt. Mater. **10**, 2102565 (2022).
21. N. Tavakoli, R. Spalding, A. Lambertz, P. Koppejan, G. Gkantzounis, C. Wan, R. Röhrich, E. Kontoleta, A. F. Koenderink, R. Sapienza, M. Florescu, and E. Alarcon-Llado, "Over 65% sunlight absorption in a 1 μm Si slab with hyperuniform texture," ACS Photon. **9**, 1206–1217 (2022).
22. É. Chéron, S. Félix, J.-P. Groby, V. Pagneux, and V. Romero-García, "Wave transport in stealth hyperuniform materials: the diffusive regime and beyond," Appl. Phys. Lett. **121**, 061702 (2022).
23. M. A. Klatt, P. J. Steinhardt, and S. Torquato, "Wave propagation and band tails of two-dimensional disordered systems in the thermodynamic limit," Proc. Natl. Acad. Sci. USA **119**, e2213633119 (2023).
24. O. U. Uche, F. H. Stillinger, and S. Torquato, "Constraints on collective density variables: two dimensions," Phys. Rev. E **70**, 046122 (2004).
25. R. D. Batten, F. H. Stillinger, and S. Torquato, "Classical disordered ground states: super-ideal gases, and stealth and equi-luminous materials," J. Appl. Phys. **104**, 033504 (2008).
26. G. Zhang, F. Stillinger, and S. Torquato, "Ground states of stealthy hyperuniform potentials: I. Entropically favored configurations," Phys. Rev. E **92**, 022119 (2015).
27. S. Torquato, G. Zhang, and F. H. Stillinger, "Ensemble theory for stealthy hyperuniform disordered ground states," Phys. Rev. X **5**, 021020 (2015).
28. W. Zhou, Y. Tong, X. Sun, and H. K. Tsang, "Ultra-broadband hyperuniform disordered silicon photonic polarizers," IEEE J. Sel. Top. Quantum Electron. **26**, 8201109 (2020).
29. M. A. Klatt, J. Kim, and S. Torquato, "Cloaking the underlying long-range order of randomly perturbed lattices," Phys. Rev. E **101**, 032118 (2020).
30. A. Sheremet, R. Pierrat, and R. Carminati, "Absorption of scalar waves in correlated disordered media and its maximization using stealth hyperuniformity," Phys. Rev. A **101**, 053829 (2020).
31. S. Torquato and J. Kim, "Nonlocal effective electromagnetic wave characteristics of composite media: beyond the quasistatic regime," Phys. Rev. X **11**, 021002 (2021).
32. J. Elser, V. A. Podolskiy, I. Salakhutdinov, and I. Avrutsky, "Nonlocal effects in effective-medium response of nanolayered metamaterials," Appl. Phys. Lett. **90**, 191109 (2007).
33. Y. Bhattacharjee, I. Arief, and S. Bose, "Recent trends in multi-layered architectures towards screening electromagnetic radiation: challenges and perspectives," J. Mater. Chem. C **5**, 7390–7403 (2017).
34. S. A. Maier, *Plasmonics: Fundamentals and Applications* (Springer, 2007).
35. U. Hohenester, *Nano and Quantum Optics* (Springer, 2020).
36. P. W. Anderson, "Absence of diffusion in certain random lattices," Phys. Rev. **109**, 1492–1505 (1958).
37. A. R. McGurn, K. T. Christensen, F. M. Mueller, and A. A. Maradudin, "Anderson localization in one-dimensional randomly disordered optical systems that are periodic on average," Phys. Rev. B **47**, 13120–13125 (1993).
38. P. Sheng, *Introduction to Wave Scattering, Localization and Mesoscopic Phenomena* (Academic, 1995).
39. C. M. Aegerter and G. Maret, "Coherent backscattering and anderson localization of light," in *Progress in Optics* (Elsevier, 2009), Vol. **52**, pp. 1–62.
40. F. M. Izrailev, A. A. Krokhin, and N. M. Makarov, "Anomalous localization in low-dimensional systems with correlated disorder," Phys. Rep. **512**, 125–254 (2012).
41. D. S. Wiersma, "Disordered photonics," Nat. Photonics **7**, 188–196 (2013).
42. H. H. Sheinfux, I. Kaminer, A. Z. Genack, and M. Segev, "Interplay between evanescence and disorder in deep subwavelength photonic structures," Nat. Commun. **7**, 12927 (2016).
43. A. Salandrino and N. Engheta, "Far-field subdiffraction optical microscopy using metamaterial crystals: theory and simulations," Phys. Rev. B **74**, 075103 (2006).
44. Y. Xiong, Z. Liu, and X. Zhang, "Projecting deep-subwavelength patterns from diffraction-limited masks using metal-dielectric multilayers," Appl. Phys. Lett. **93**, 111116 (2008).
45. S. Oh, J. Kim, X. Piao, S. Kim, K. Kim, S. Yu, and N. Park, "Control of localization and optical properties with deep-subwavelength engineered disorder," Opt. Express **30**, 28301–28311 (2022).
46. P. Yeh, *Optical Waves in Layered Media* (Wiley, 2005).

47. S. Rytov, "Electromagnetic properties of a finely stratified medium," Sov. Phys. JEPT **2**, 466–475 (1956).
48. D. Sjöberg, "Exact and asymptotic dispersion relations for homogenization of stratified media with two phases," J. Electromagn. Waves Appl. **20**, 781–792 (2006).
49. A. Maurel and V. Pagneux, "Effective propagation in a perturbed periodic structure," Phys. Rev. B **78**, 052301 (2008).
50. A. V. Chebykin, A. A. Orlov, A. V. Vozianova, S. I. Maslovski, Y. S. Kivshar, and P. A. Belov, "Nonlocal effective medium model for multilayered metal-dielectric metamaterials," Phys. Rev. B **84**, 115438 (2011).
51. V. Popov, A. V. Lavrinenko, and A. Novitsky, "Operator approach to effective medium theory to overcome a breakdown of Maxwell Garnett approximation," Phys. Rev. B **94**, 085428 (2016).
52. A. M. Merzlikin and R. S. Puzko, "Homogenization of Maxwell's equations in a layered system beyond the static approximation," Sci. Rep. **10**, 15783 (2020).
53. Z. Wen, H. Xu, W. Zhao, Z. Zhou, X. Li, S. Li, J. Zhou, Y. Sun, N. Dai, and J. Hao, "Nonlocal effective-medium theory for periodic multilayered metamaterials," J. Opt. **23**, 065103 (2021).
54. S. Torquato, *Random Heterogeneous Materials: Microstructure and Macroscopic Properties* (Springer, 2002).
55. P. Debye, H. R. Anderson, and H. Brumberger, "Scattering by an inhomogeneous solid. II. The correlation function and its applications," J. Appl. Phys. **28**, 679–683 (1957).
56. S. Torquato, "Inverse optimization techniques for targeted self-assembly," Soft Matter **5**, 1157–1173 (2009).
57. L. Tsang and J. A. Kong, "Scattering of electromagnetic waves from random media with strong permittivity fluctuations," Radio Sci. **16**, 303–320 (1981).
58. T. G. Mackay, A. Lakhtakia, and W. S. Weiglhofer, "Third-order implementation and convergence of the strong-property-fluctuation theory in electromagnetic homogenization," Phys. Rev. E **64**, 066616 (2001).
59. M. C. Rechtsman and S. Torquato, "Effective dielectric tensor for electromagnetic wave propagation in random media," J. Appl. Phys. **103**, 084901 (2008).
60. V. M. Agranovich and Y. N. Gartstein, "Spatial dispersion and negative refraction of light," Phys. Usp. **49**, 1029–1044 (2006).
61. B. X. Wang and C. Y. Zhao, "Achieving a strongly negative scattering asymmetry factor in random media composed of dual-dipolar particles," Phys. Rev. A **97**, 023836 (2018).
62. L. Tsang, *Scattering of Electromagnetic Waves*, Wiley Series in Remote Sensing (Wiley, 2001).
63. K. Vynck, R. Pierrat, R. Carminati, L. S. Froufe-Pérez, F. Scheffold, R. Sapienza, S. Vignolini, and J. J. Sáenz, "Light in correlated disordered media," arXiv, arXiv: 2106.13892 (2021).
64. S. Torquato, "Hyperuniformity and its generalizations," Phys. Rev. E **94**, 022122 (2016).
65. J. D. Jackson, *Classical Electrodynamics* (Wiley, 1990).
66. G. Zhang, F. H. Stillinger, and S. Torquato, "Can exotic disordered 'stealthy' particle configurations tolerate arbitrarily large holes?" Soft Matter **13**, 6197–6207 (2017).
67. A. Taflove, S. G. Johnson, and A. Oskooi, *Advances in FDTD Computational Electrodynamics: Photonics and Nanotechnology* (Artech House, 2013).
68. A. F. Oskooi, D. Roundy, M. Ibanescu, P. Bermel, J. D. Joannopoulos, and S. G. Johnson, "MEEP: a flexible free-software package for electromagnetic simulations by the FDTD method," Comput. Phys. Commun. **181**, 687–702 (2010).
69. G. W. Milton, D. J. Eyre, and J. V. Mantese, "Finite frequency range Kramers-Kronig relations: bounds on the dispersion," Phys. Rev. Lett. **79**, 3062–3065 (1997).
70. E. Nichelatti, "Complex refractive index of a slab from reflectance and transmittance: analytical solution," J. Opt. A **4**, 400–403 (2002).
71. M. A. Klatt, P. J. Steinhardt, and S. Torquato, (2023), in preparation.
72. J. D. Affinito, M. E. Gross, C. A. Coronado, G. L. Graff, I. N. Greenwell, and P. M. Martin, "A new method for fabricating transparent barrier layers," Thin Solid Films **290**–291, 63–67 (1996).
73. S.-S. Lee, J.-D. Hong, C. H. Kim, K. Kim, J. P. Koo, and K.-B. Lee, "Layer-by-layer deposited multilayer assemblies of ionene-type polyelectrolytes based on the spin-coating method," Macromolecules **34**, 5358–5360 (2001).
74. J. R. Tumbleston, D. Shirvanyants, N. Ermoshkin, R. Janusziewicz, A. R. Johnson, D. Kelly, K. Chen, R. Pinschmidt, J. P. Rolland, A. Ermoshkin, E. T. Samulski, and J. M. DeSimone, "Continuous liquid interface production of 3D objects," Science **347**, 1349–1352 (2015).

140.180.240.58 {ts '2023-07-25 10:40:06'}